Investigations on the fouling characteristic of humic acid and alginate sodium in capacitive deionization

Huizhong Zhang, Jiayu Tian, Xiujuan Hao, Dongmei Liu and Fuyi Cui

ABSTRACT

Capacitive deionization (CDI) has been investigated for brackish water desalination, selective removal of ions, and water softening. We used humic acid (HA) and alginate sodium (SA) to simulate different kinds of natural organic matter to investigate the fouling phenomena during CDI operation. Adsorption amount and energy efficiency were studied. Results showed that both SA and HA could decrease the removal of NaCl during CDI operation. There existed a slight decrease of energy consumption in SA solutions which was opposite to that in HA solutions. HA can compete with ions adsorbed by electrodes and attach to electrodes adhesively, resulting in co-ion repulsion. SA is not sensitive to electrical field and its fouling is not obvious. The amount of adsorbed Mg^{2+} would increase from 0.927 mg/g to 1.508 mg/g in ten cycles' operation and the increment of Ca^{2+} was from 1.885 mg/g to 2.878 mg/g in SA solutions. This increase of adsorption was due to the complexation between SA and cations. Simultaneously, energy consumption was decreased. In HA solutions, energy consumption of Mg^{2+} and Ca^{2+} adsorption increased. In ten cycles' operations, both HA and SA could reduce the efficiency of CDI operation. The types of organic substances are important factors in fouling of CDI electrodes.

Key words | alginate sodium, capacitive deionization, fouling, humic acid

HIGHLIGHTS

- The mechanisms of humic acid and sodium alginate fouling were investigated in CDI operation.
- Humic acid was able to make fouling of electrodes worse during CDI operation.
- Alginate sodium acted as a medium in increasing the amount of adsorption and energy efficiency.

Huizhong Zhang
Jiayu Tian (corresponding author)
Xiujuan Hao
Dongmei Liu
School of Environment, Harbin Institute of Technology,
Harbin 150090,
China
E-mail: *tjy800112@163.com*

Jiayu Tian
School of Civil Engineering and Transportation,
Hebei University of Technology,
Tianjin 300401,
China

Fuyi Cui
Chongqing University,
Chongqing 400044,
China

doi: 10.2166/wrd.2021.104

GRAPHICAL ABSTRACT

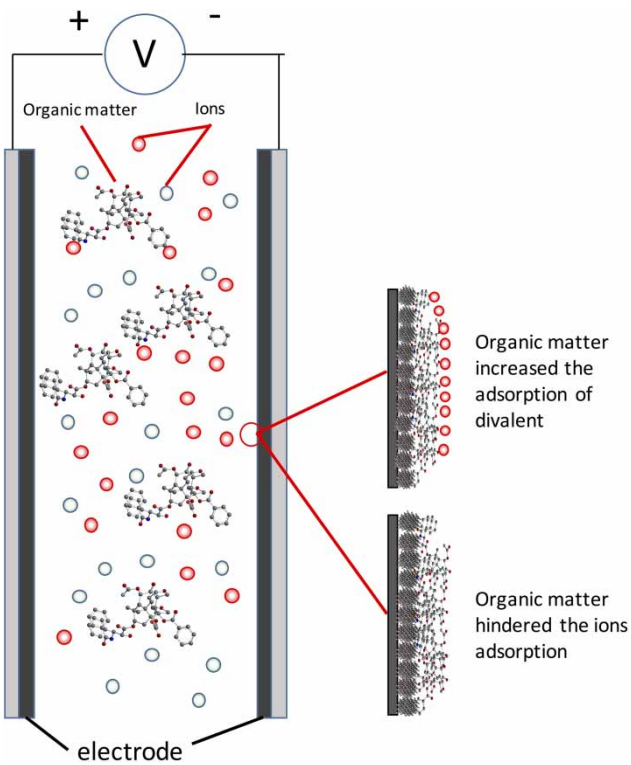

INTRODUCTION

Water scarcity posts a great challenge to the development of human society, industry, and agriculture. Desalination of brackish water and wastewater reuse are effective ways to increase the supply of clean water (Xu *et al.* 2019). Nowadays, reverse osmosis (RO), electrodialysis (ED), and vacuum membrane distillation are common methods of water treatment and desalination (Zhu *et al.* 2019). These techniques mostly have high energy requirements and may be not very efficient in desalination of medium-low salt water. In recent years, capacitive deionization (CDI) has attracted the interest of researchers for its comparatively low energy cost, easy regeneration and energy reclaim which also can be applied for selective removal of ions and water softening (Alfredy *et al.* 2019).

CDI usually works at a low voltage (lower than 2 V) in order to avoid water electrolysis. Similar to a capacitor, the voltage is applied between two parallel electrodes. In the desalination step, the movement of ions in salinity water is driven by a direct electric field. Because of electrostatic interaction, salt ions are adsorbed by electrodes with the opposite charges. They will be stored in micropores and mesopores of electrodes and form layers which are called the electrical double layers (EDLs). The adsorption amount of ions mainly depends on the thickness of EDLs. Then, the regeneration process was operated at 0 V, which is called short-circuit, or by supplying an opposite voltage (Choi *et al.* 2017). Adsorbed ions are desorbed from electrodes.

Since the deslination process mainly depends on the formation of EDLs in micropores and mesopores, the pore structure of electrodes has a great influence on salt removal efficiencies (Dykstra *et al.* 2016). Thus, the electrode materials are very important for the efficiencies of CDI. Usually, materials for electrode preparation should have

plenty of mesopores and micropores, high surface areas, and high electrical conductivity. Carbon materials are ideal materials. Activated carbon, carbon fiber, mesoporous carbon, carbon nanotube, and graphene are often applied in preparing electrodes. These materials have some shortcomings in practical application. Some carbon materials are hydrophobic, thus it is very difficult for the salty water to go inside the pores. Some materials are very expensive and preparations of a lot of materials are too complicated. Some materials have low adsorption capacity of salts.

As a result, many studies have focused on developing new electrode materials. Fang *et al.*'s (2016) study used hydrophobic polyurethane elastomer as binder for preparing electrodes. This made the adsorption process more stable compared to traditional binder. Wang *et al.* (2012) prepared carbon nanofiber by electrospinning and achieved an improvement in adsorption amount. Tsai & Doong (2015) made hierarchically ordered mesoporous carbons and this material could get fast adsorption in grey and brown water treatment. These materials actually help increase the salt removal efficiencies of CDI. However, their applications in practical water treatment have not been investigated clearly.

The concentration of salt in environmental water often ranges from 1,000 mg/L to 10,000 mg/L. The concentrations of organic matter are about 1–21 mg/L as DOC (dissolved organic carbon) (Liu *et al.* 2018). During CDI operation, organic substances are inevitably in contact with carbon electrodes. Meanwhile, the carbon materials are also great adsorbents for other organic and inorganic substances. Once the electrodes adsorb the organic matter during the desalination process, properties like surface area and functional groups of carbon materials might be altered (Tang *et al.* 2014). Desalination efficiencies of some materials in CDI operation remain unknown in water with organic matter. In addition, the heterogeneous and complicated organic molecules can easily interact with cations and anions, thus affecting the transport of ions. To make the best use of some new materials in CDI operation, the impact caused by organic matter on desalination efficiencies should be found out. A large amount of new materials have been reported and there are many kinds of organic matter in practical water. Investigating this organic matter and materials at one time may be too complicated. We could first investigate the fouling phenomena and mechanisms caused by various organic matter with the help of common materials. These studies could help us predict and understand the fouling of new materials.

In this study, we used the common material activated carbon (AC) to systematically investigate the fouling mechanisms of humic acid HA and alginate sodium SA in CDI operation. HA and SA are typical organics of humic substances and polysaccharides to study the influence of organic fouling. We also studied the fouling phenomena in solutions of monovalent ions (NaCl) and divalent ions ($MgCl_2$ and $CaCl_2$). The effect of fouling was assessed by adsorption efficiency and energy consumption. SEM images and FTIR spectroscopy were applied to investigate fouling on electrodes. The interactions between organic matter and ions were compared during CDI operation. This research would help to understand the fouling phenomena on carbon materials' electrodes. It could also give some worthwhile information on CDI operation and influent water pre-treatment in practical water desalination.

MATERIALS AND METHODS

Chemical reagents and feed solution composition

NaCl, $CaCl_2$, and $MgCl_2$ are chosen to simulate the salinity of the water. The composition of feed solutions is shown in Table 1. Before the experiments, the solutions were stirred overnight to make them stable and homogeneous. Then, they were filtered through a 0.45 μm cellulose acetate membrane. The pH of the solutions was adjusted to 7. Deionized water (DI) is used throughout our experiments.

Preparation of electrodes

The commercial activated carbon (AC) (Sigma-Aldrich) powder was used to fabricate electrodes. To prepare carbon electrodes, AC, graphite (Sigma-Aldrich) as conductive material and poly (vinylidene fluoride) (PVDF) (Sigma-Aldrich) powders were mixed together at a mass ratio of 8:1:1. Then, some drops of N-methyl pyrrolidone (Aladdin) were added to make the powder slurry. The slurry was stirred for about 8 h to make it more homogeneous. The resulting slurry was coated on a graphite sheet strip with a

Table 1 | Composite of feed solutions

	Parameters		
Solutions	**NaCl (mg/L)**	**Humic acid (mg/L)**	**Alginate sodium (mg/L)**
S1	200	–	–
S2	200	50	–
S3	200	20	–
S4	200	–	50
S5	200	–	20
	$MgCl_2$ (mg/L)	**Humic acid (mg/L)**	**Alginate sodium (mg/L)**
S6	200	–	–
S7	200	20	–
S8	200	–	20
	$CaCl_2$ (mg/L)	**Humic acid (mg/L)**	**Alginate sodium (mg/L)**
S9	200	–	–
S10	200	20	–
S11	200	–	20
S12	–	20	–
S13	–	–	20

size of 10×4 cm. The sheets with carbon slurry were then dried in the oven at 120 °C for 2 h and then put in a vacuum oven at 80 °C for 2 h to remove the organic solvent completely. Each electrode weighed about 0.5 g and had a thickness of 200–300 μm.

Reactor configuration

CDI experiments were conducted in a flow-through system. The system consisted of a CDI unit cell, a reservoir, a peristaltic pump, and a conductivity meter. The CDI unit cell was composed of a pair of parallel activated carbon electrodes separated by a 1 mm gap. This gap could prevent a short circuit and allow liquid to flow. The electrodes were placed in plexiglass housing which had two endplates with silicone rubber sheets as gasket. Both plexiglass endplates had holes to allow water to flow. The flow rate was about 15 mL/min. The pump drove the feed solution flowing from the reservoir to the lower inlet hole of the endplate. The feed solution flew through the spacer gap between the electrodes. The total volume of solution in the reservoir was 100 mL. Then, the effluent left from the upper hole of the other endplate and flowed into the reservoir. A voltage of 1.2 V was applied between the parallel electrodes by a workstation (CHI660D, CH Instruments, Inc.) and the corresponding current was recorded. An online conductivity meter was applied to monitor the conductivity of solution in the reservoir. No pH adjustment for the solutions was carried out throughout the CDI operation. A complete CDI operation included two steps: adsorption and desorption (regeneration). In our experiments, the adsorption process took 1,300 s. Desorption, which was also called regeneration, lasted 1,100 s at a cell potential of 0 V. A cycle included one adsorption step and one desorption step. Before each cycle started, solution in the reservoir would be changed to a new one.

Experimental methods

The CDI device was carried out for ten cycles to investigate the effects of organic substances on deionization. The fouling was monitored mainly by the salt adsorption amount and energy consumption efficiency. CDI efficiencies were calculated by the changes of the ion amounts in the feed solutions. The initial and equilibrium concentrations were detected in every cycle. The salt adsorption amount per cycle (q, mg/g) was calculated according to Equation (1):

$$q = \frac{C_0 \cdot V - C_t \cdot V}{m} \tag{1}$$

where C_0 and C_t are the initial and equilibrium concentrations (mg/L), respectively. V is the volume of solution (L), and m is the weight of the electrodes (g). The total energy consumption (W) of an adsorption step was calculated by Equation (2) and energy consumption efficiency (Wq) of the CDI unit cells was calculated using Equation (3) (Chen *et al.* 2018):

$$W = \frac{U \int_0^t I dt}{3600m} \tag{2}$$

where W is the energy consumption (Wh), U is the applied voltage (V), I is the correspondent current (A) and t is adsorption time (s):

$$Wq = \frac{1000W}{q} \tag{3}$$

Also, in some experiments, the carbon electrodes were used to contact with organic matter before conducting the CDI process. The adsorption of SA and HA was performed individually at a voltage of 1.2 V for 2 h, 10 h, and 4 days. Then pre-fouled electrodes were used in CDI operation.

Analysis

Conductivity and concentration analysis

The changes in the conductivity of solutions were analyzed by a conductivity meter (DDSJ-308A, Leici company). Cation concentrations were determined by inductive couple plasma optical emission spectrometry (ICP-OES, Perkin Elmer Optima 5300DV). In NaCl solutions, the concentrations of NaCl were detected via the concentrations of chloride ions. Anion concentrations were determined by ion chromatography (883-basic IC plus, Metrohm). In addition, the variation of the organic matter was also detected. The concentrations of HA were measured by a UV-Vis spectrophotometer (Beijing Puxi, T6) at a wavelength of 254 nm. Alginate sodium was determined using the phenol-sulfuric acid colorimetric method at 490 nm (Xie *et al.* 2013).

Characterization of electrodes and particles in solutions

Zeta potentials and nanoparticle size were detected with Zetasizer nano ZS (Malvern, Nano-Z) at 25 °C. Solutions with organic matter and different cations were investigated. Solutions for ζ-potential and nanoparticle detecting were adjusted to different pH values by NaOH and HCl. All the samples were shaken for 24 h. pH would be determined again before measuring the zeta potential and nanoparticle size. We studied the fresh and fouled electrodes using Fourier transform infrared spectroscopy (Spotlight 400, Pekin-Elmer, USA). The morphology of fresh and fouled electrodes was studied by SEM (SUPRA55, ZEISS, Germany).

Electrochemical analysis

Electrochemical properties of electrodes were evaluated using a CHI660D electrochemical workstation (Shanghai Chenhua Instruments Co., China) in a three-electrode system at 25 °C. The Ag/AgCl electrode was used as the reference electrode and a piece of platinum foil was used as the counter electrode. The working electrode was activated carbon electrode. Prior to the tests, adsorption experiments were conducted at a voltage of 1.2 V for 10 h in $CaCl_2$ or $MgCl_2$ solutions with organic substances. The cyclic voltammetry (CV) of electrodes was investigated at the scan rate of 50 mV/s in solutions containing 5 mM $CaCl_2$ or $MgCl_2$ and 200 mg/L of SA or HA. The potential was set between −0.4 and 0.6 V. The specific capacitance was calculated from Equation (4) (Hou & Huang 2013):

$$C = \frac{\int IdV}{2vm\Delta V} \tag{4}$$

where C (F) is the specific capacitance, I (A) is the response current density, ΔV (V) is the potential window, v (V/s) is the scan rate, and m (g) is the mass of the electrode material.

RESULTS AND DISCUSSION

ζ-potential and nanoparticle size of organic substances molecules

Foulants in environmental water can be categorized into different kinds, such as humic substances, polysaccharides, and protein. The typical humic substance is humic acid. HA is a kind of hydrophobic organic acid (Chen *et al.* 2018). It contains abundant functional groups, for example, aromatic nucleus. Alginate sodium (SA), which consists of β-D-mannuronic and α-L-guluronic acids, is a kind of hydrophilic organic matter and is a typical polysaccharide substance (Lee & Mooney 2012). In this study, these two substances act as the natural organic substances in the water. The measured ζ-potentials of HA and SA are shown in Figure 1(a). It was found that both HA and SA had negative ζ-potentials at all pH ranging from 3 to 10. HA and SA are macromolecule organic substances with numerous functional groups like carboxylic and oxhydryl groups which make them soluble in water and have negative charge (Lee & Mooney 2012; Tang *et al.* 2014). The potential of HA was about −15 mV to −25 mV and that of SA was about −5 mV to −15 mV. This demonstrates that HA produced more charges and could be easily driven by electrostatic force. After the addition of

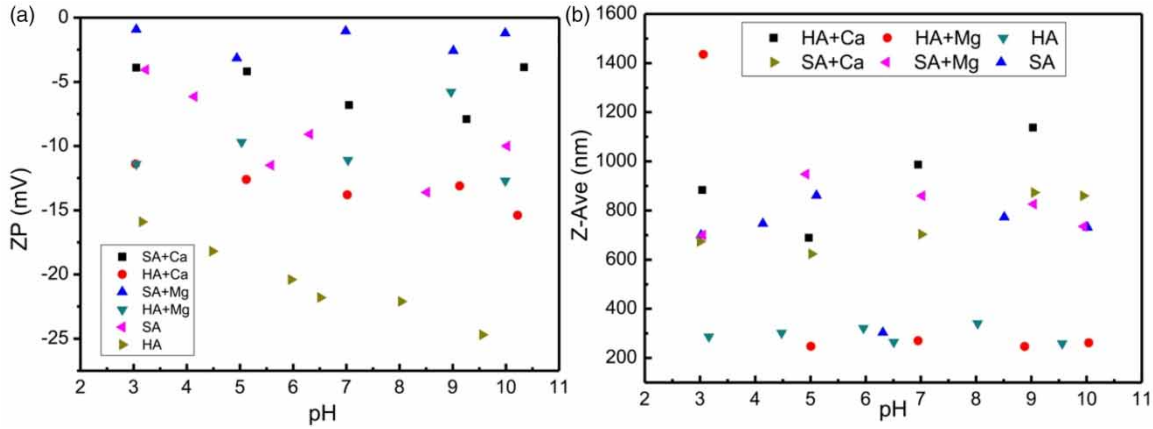

Figure 1 | ζ-potential and nanoparticle size of HA and SA at various solution pH and in different solutions.

divalent cations, ζ-potential turned to the positive direction gradually. Both Ca^{2+} and Mg^{2+} could interact with HA and SA forming complexes (Alberts & Filip 1998; Topuz *et al.* 2012). The cations complexed on organic molecules can neutralize the negative charges.

Simultaneously, the nanoparticle size was also analyzed and shown in Figure 1(b). SA had larger particle size than HA. Alginate is a kind of anioinic polymer and has a liner structure (Lee & Mooney 2012). HA has a curled molecular structure resulting from the inner electrostatic interaction. The divalent cations complexed with HA molecules and made the curled molecular stretched (Yang *et al.* 2011). The complexation might hinder the mobility of ions. In SA solutions, the urionic acid on SA made it interact easily with divalent cations and gelation. The gelation captures cations in water leading to reduction of free ions in solutions which can easily be mobilized in the electrical field and be adsorbed by electrodes. The gel can attach to electrodes, slowing down the transmission of ions.

NaCl adsorption efficiency with and without organic substances

NaCl adsorption efficiency

We investigated the adsorption of NaCl with and without organic substances. The conductivity during the experiments was recorded (Figure 2). The concentration of NaCl was directly proportional to the conductivity. The changes of conductivity could represent the variation of the concentration of NaCl in the solutions. When the voltage of 1.2 V was applied, electrodes adsorbed ions and the conductivity of the NaCl solution dropped. When the conductivity was stable, the adsorption step ended. Then, the desorption step started and adsorbed ions were desorbed from electrodes and conductivity began to decrease. As the number of cycles increased, the variation of conductivity was quite different from that in the first cycle. Especially in the ninth and tenth cycles, when the voltage was applied, conductivity was increased instead of dropping. This was due to the fact that ions absorbed by electrodes could not be removed totally at each regeneration step and some ions might be absorbed by electrodes freely no matter what kind of charges they brought at the regeneration step. When the next adsorption step started, ions, bringing the same charges with the electrodes would go back to water driven by repulsive force. This phenomenon was called co-ion repulsion and it often happened in CDI operation. Co-ion repulsive force could consume the energy provided by the voltage of 1.2 V which should have been used for deionization, leading to the decrease of the adsorption amount in the next cycle. From the experiments in S2 and S3, it can be seen that HA in water could enhance the co-ion repulsion. In solution S2, co-ion repulsion could be observed in five cycles. In S3, only in three cycles did the co-ion repulsion take place. Due to the higher concentration of HA, co-ion repulsion became obvious. In S4 and S5, a similar phenomenon was observed. SA also enhanced the co-ion repulsion

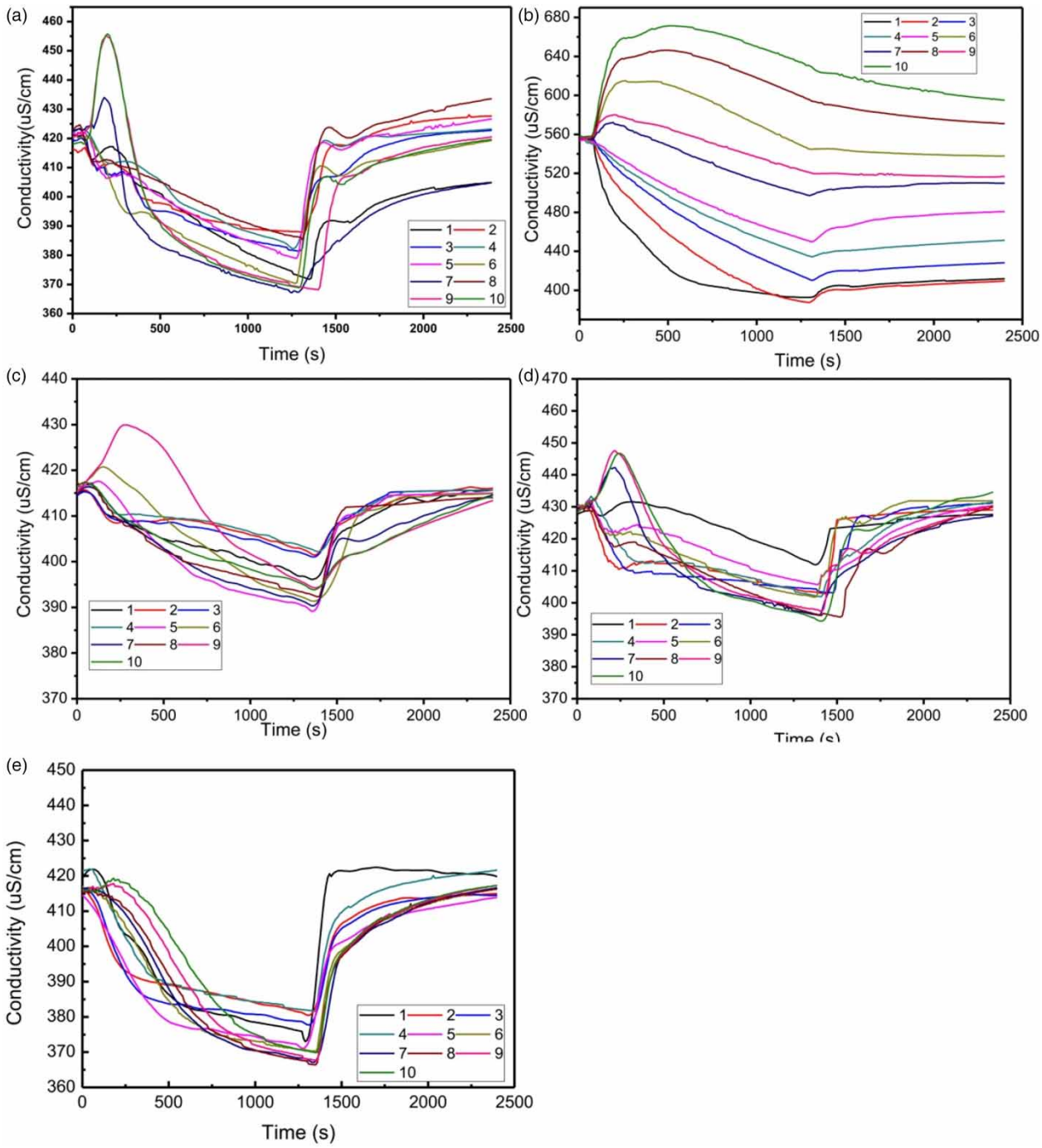

Figure 2 | The variation of conductivity and concentration in NaCl solutions with different constituents: (a) S1, (b) S2, (c) S3, (d) S4, (e) S5.

during the adsorption step. These results showed that with the concentration of organic substances increasing, co-ion repulsion was enhanced. However, in SA fouling, co-ion repulsion was not as severe as that in HA fouling.

Figure 3 exhibits the salt adsorption amount per cycle in different kinds of NaCl solutions. Salt adsorption in pure NaCl solution is from 6.87 mg/g to 2.62 mg/g. There was a reduction of the adsorption amount in pure solution because

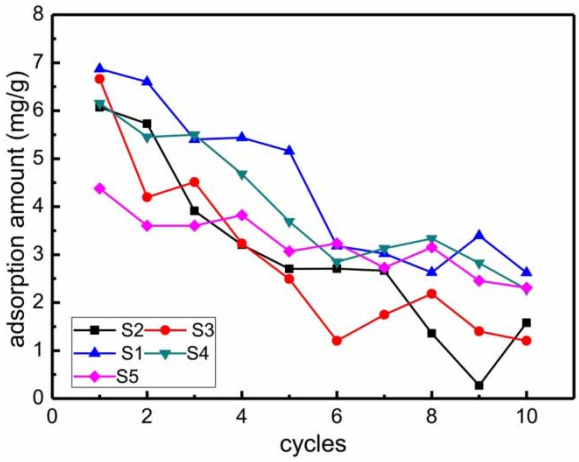

Figure 3 | The salt adsorption amount in different solutions during ten cycles.

of the inevitable redox reaction on electrodes (Lu *et al.* 2017), which would change functional groups on electrodes. These functional groups could adsorb more ions during the generation step and lead to co-ion repulsion. In pure NaCl solution, the adsorption amount decreased about 62%. In solutions with 50 mg/L HA, the adsorption amount decreased about 96%. In solutions with 20 mg/L HA, the adsorption amount decreased about 82%. This proved that with the increasing concentration of HA, the adsorption amount of salts was reduced faster than that in pure NaCl solution. HA had an adverse impact on salts' removal efficiencies. In solutions of 20 mg/L SA, the adsorption amount decreased 47%. In solutions of 50 mg/L SA, the adsorption amount decreased about 63%. Different from HA, the existence of SA in water did not reduce the adsorption amount of salts too much. From these results, it can be concluded that the existence of some organic substances clearly reduces the deionization of the CDI process. With the concentration of HA increasing, the adverse impact became obvious. HA would lead to more severe fouling than SA. From Figure 1, both HA and SA have negative ζ-potential in water. The organic matter competed with NaCl ions in water adsorbed by electrodes. A part of the energy was consumed by the adsorption of organic substances. Because SA produced fewer charges, the competition between organic matter and ions was weakened. SA was a kind of hydrophilic organic matter. Adsorption of SA could make the electrodes hydrophilic. Also, salty water could easily get inside the pores of electrodes.

Effect of voltage on adsorption of organic substances

HA has lower ζ-potential than SA dosage, meaning that HA has stronger electrostatic attraction. Figure 4 shows the effect of voltage on adsorption of organic matter. In HA solution, the adsorption amount was from 0.412 mg/g to 0.161 mg/g at voltage of 1.4 V. At 1.2 V, the adsorption amount of HA decreased to 0.173–0 mg/g and at 1.0 V, the adsorption amount was stable with 0.112 mg/g to 0 mg/g. There are many interactions between the organic substances and adsorbents, such as π-π bonding, hydrophobic interactions, and electrostatic interactions (Yang & Xing 2009). The adsorption of organic matter on carbon-based adsorbents was affected by

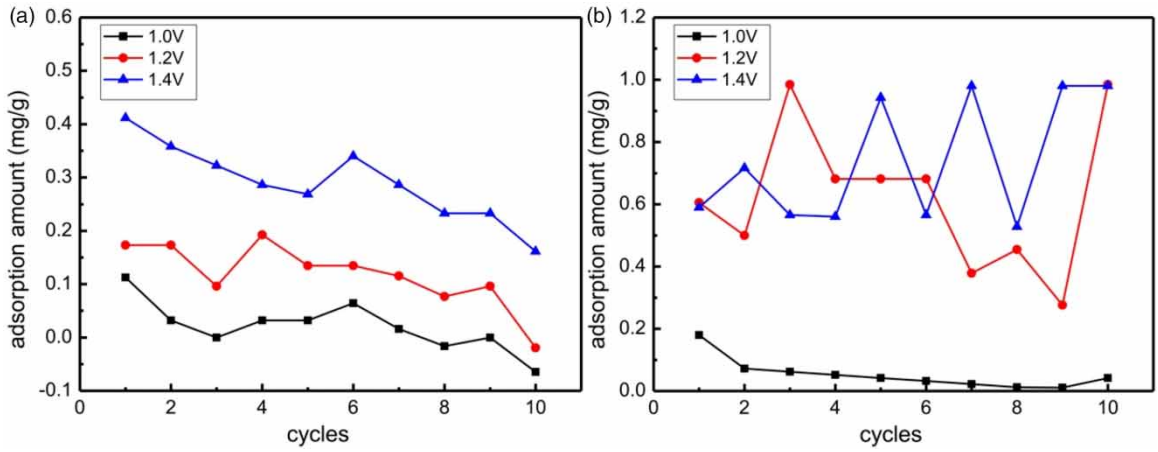

Figure 4 | Adsorption amount of HA and SA in electric field: (a) S12, (b) S13.

the water quality, the contaminants, and properties of adsorbents. The results from our work demonstrated that in the electrical field the dominant interaction was electrostatic force. In SA solution, at 1.0 V, the adsorption amount was nearly 0 mg/g. This proved that SA was not as sensitive as HA to voltage. The adsorption amount of SA could probably be attributed to other interactions with electrodes.

In Figure 5(a) and 5(b), it can be seen that the concentration at adsorption equilibrium was higher than that at desorption equilibrium. This meant that adsorbed organic substances hardly desorbed from the electrodes during the regeneration step. In HA solutions, the electrodes kept adsorbing organic substances during the desorption steps. This could prove that there were not only electrostatic interactions but also other interactions between organic substances and electrodes during CDI operation. Thus, HA and SA could accumulate on carbon electrodes without being desorbed from electrodes when the voltages were 0 V. The adsorbed organic substances can interact with ions in water through electrostatic force in the regeneration step (Li *et al.* 2002). This interaction makes the electrodes adsorb more ions than that in pure solution, leading to more obvious co-ion repulsion.

The adsorption amount of organic matters in solutions with salts is shown in Figure 6. Electrodes adsorbed organic matters and ions at the same time during adsorption steps. The adsorption amount of HA in S2 was about 0.58–0.22 mg/g, which was higher than that in S12. The higher concentration of HA promoted the adsorption of organic matter. Similarly, the adsorption amount of SA in S4 was higher than that in S13. The adsorption amount of HA in S3 was about 0.2 mg/g–0 mg/g and the adsorption amount of SA in S5 was about 0.6 mg/g–0.25 mg/g. There was no obvious difference between adsorption in solutions with and without salts. Although there was competition in adsorption between organic matters and salts, the other interaction forces like π-π bonding and hydrophobic interactions could help electrodes adsorb some HA and SA.

Characterization of organic fouled electrodes

To explore the foulants, we studied the fouling electrodes. The electrodes were fouled in organic solutions at 1.2 V for about 4 days to make the fouling obvious. In Figure 7(a) and 7(c), HA and SA both had stretching at about 3,350 cm^{-1} representing alcohol/phenol O-H, at about 1,560 cm^{-1} representing carboxylate C = O and at 1,250–1,500 cm^{-1} representing in-plane O-H. The bending at 1,090 cm^{-1} and 1,030 cm^{-1} represented aliphatic C-O stretching in HA and polysaccharide C-O in SA (Liu *et al.* 2018). In Figure 7(b), fouled electrodes had an obvious peak intensity at about 1,560 cm^{-1}. In Figure 7(d), a similar

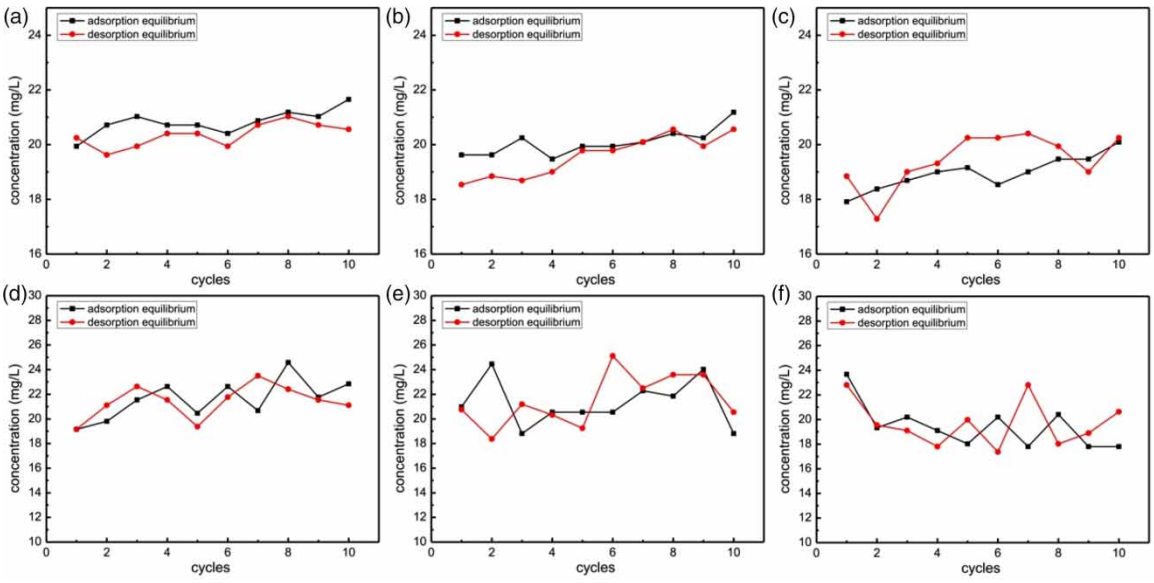

Figure 5 | The variation of concentration in HA and SA solution at voltage of 1.0 V, 1.2 V, and 1.4 V: HA solution (a) 1.0 V, (b) 1.2 V, (c) 1.4 V and SA solution (d) 1.0 V, (e) 1.2 V, (f) 1.4 V.

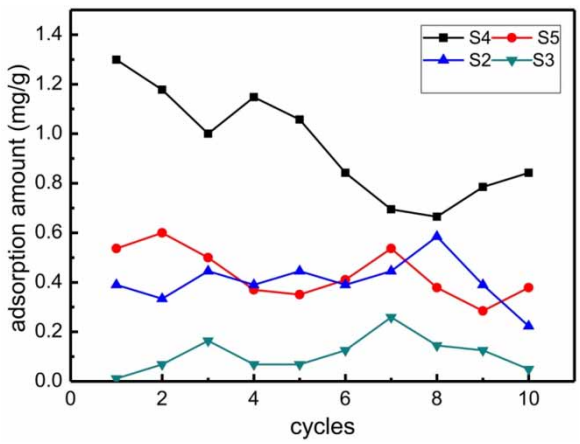

Figure 6 | The variation of HA and SA concentration in solutions with salts.

stretching is also shown. It proved that carboxylate functional groups appeared on electrodes and made them produce more negative charges in solutions. Then, the electrodes could adsorb ions during generation steps resulting in severe co-ion repulsion.

The SEM images of fresh and fouled electrodes are shown in Figure 8. With the fouling time increasing, organic matter could aggregate on electrodes. AC particles on electrodes were coated by SA and HA. The fouling layer formed on electrodes. Due to the deposition of organic matter, some micropores and mesopores on electrodes were covered.

Effect of organic fouling on energy consumption

The energy consumption efficiencies in NaCl solutions are shown in Figure 9. It can be seen that as cycles increased energy consumption efficiencies kept decreasing. In pure solution, with CDI devices running, the performance of

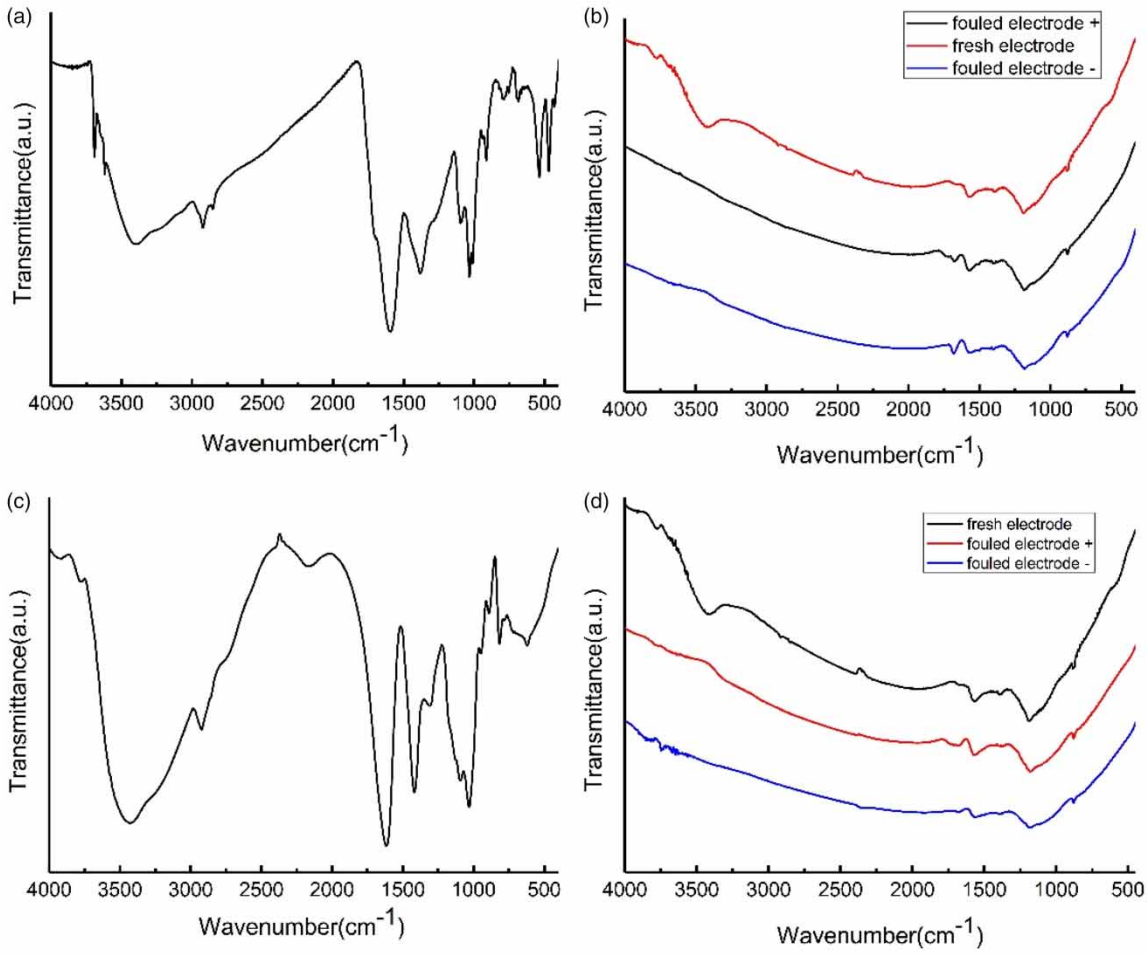

Figure 7 | FTIR spectrum of organic substances and fouled electrodes: (a) HA, (b) fouled electrodes by HA, (c) SA, (d) fouled electrodes by SA.

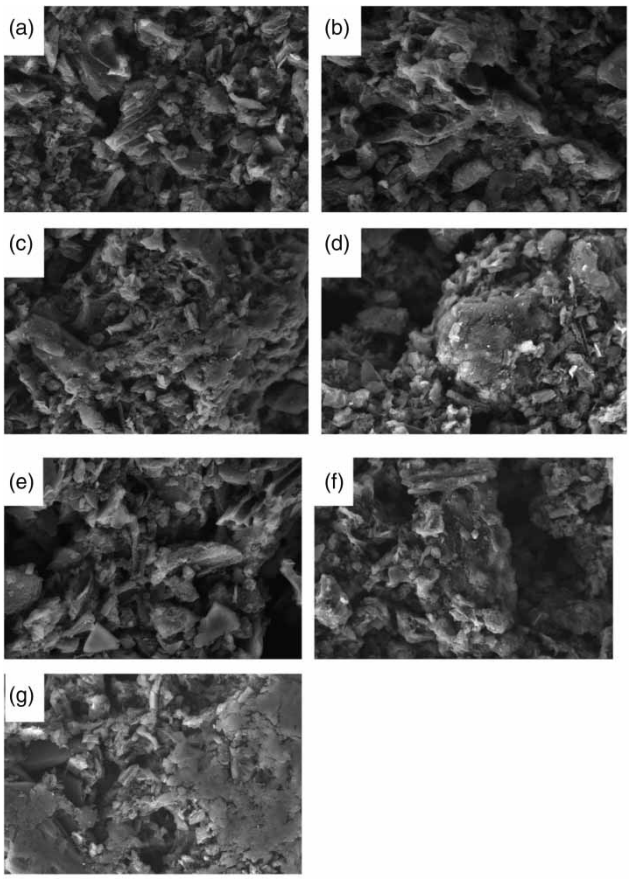

Figure 8 | The SEM images of fresh and fouled electrodes: (a) fresh electrodes, (b) 2 h HA fouling, (c) 10 h HA fouling, (d) 4 d HA fouling, (e) 2 h SA fouling, (f) 10 h SA fouling, (g) 4 d SA fouling.

electrodes was decreasing because of the inevitable redox reaction on them (Shapira *et al.* 2016). At the beginning of CDI operation, the energy efficiencies in S1 solution was 1.4637 Wh/g higher than that in organic matter solutions of around 0.82 Wh/g. In HA solution, the energy consumption efficiency rose sharply to nearly 5 Wh/g, which was much higher than efficiency in pure NaCl and SA solutions. In SA solution, the efficiency substantially increased from 0.8279 Wh/g to 2.1175 Wh/g. At the beginning, conductivities of S2 and S3 were a little bit higher than that of pure solution, possibly due to dissolution of organic substances. Higher conductivity helped reduce the resistance of solution leading to lower energy consumption on the solution. At the end of CDI operation, a certain amount of HA in water accumulated on electrodes resulting in obvious co-ion repulsion which wastes too much energy.

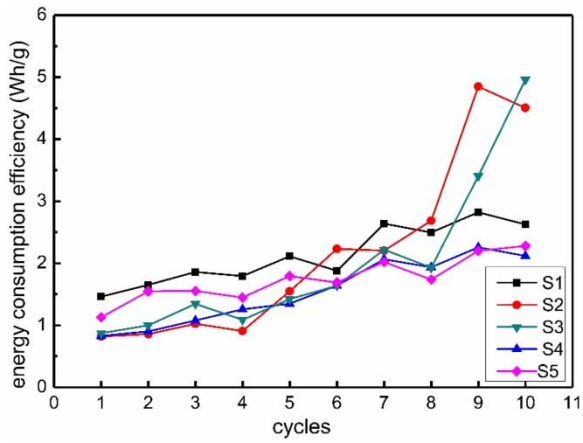

Figure 9 | Energy consumption efficiency in NaCl solutions.

In the electrical field, the dominant interaction between organic substances and electrodes was electrostatic force. Organic substances in water competed with NaCl ions during the deionization process and decreased the adsorption amount of NaCl ions. The adsorbed organic substances, like HA, enhanced co-ion repulsion. These two interactions raised the energy consumption during the deionization process. Different to HA, SA molecules have higher ζ-potential than HA molecules. Alginate did not attach to electrodes as adhesively as HA did. SA in solutions helped increase the conductivity in water and decrease the resistance of solutions leading to lower energy consumption than that in pure NaCl. Also, SA attached to the electrodes and made it become hydrophilic.

$Mgcl_2$ and $CaCl_2$ adsorption efficiency with and without organic substances

$Mgcl_2$ and $CaCl_2$ adsorption efficiency

The variations of $MgCl_2$ and $CaCl_2$ concentrations in pure solutions are demonstrated in Figure 10(b) and 10(d). There was no significant difference in the adsorption of Mg^{2+} and Ca^{2+} between the ten cycles. This could be explained by the fact that Mg^{2+} and Ca^{2+} both had a larger hydrated radius than did Na^{+} (Hou & Huang 2013). Ca^{2+} and Mg^{2+} could not enter into micropores of electrodes. They could be desorbed easily in regeneration steps. In $CaCl_2$ solutions, apparent co-ion repulsion was also observed. The calcium hydroxide

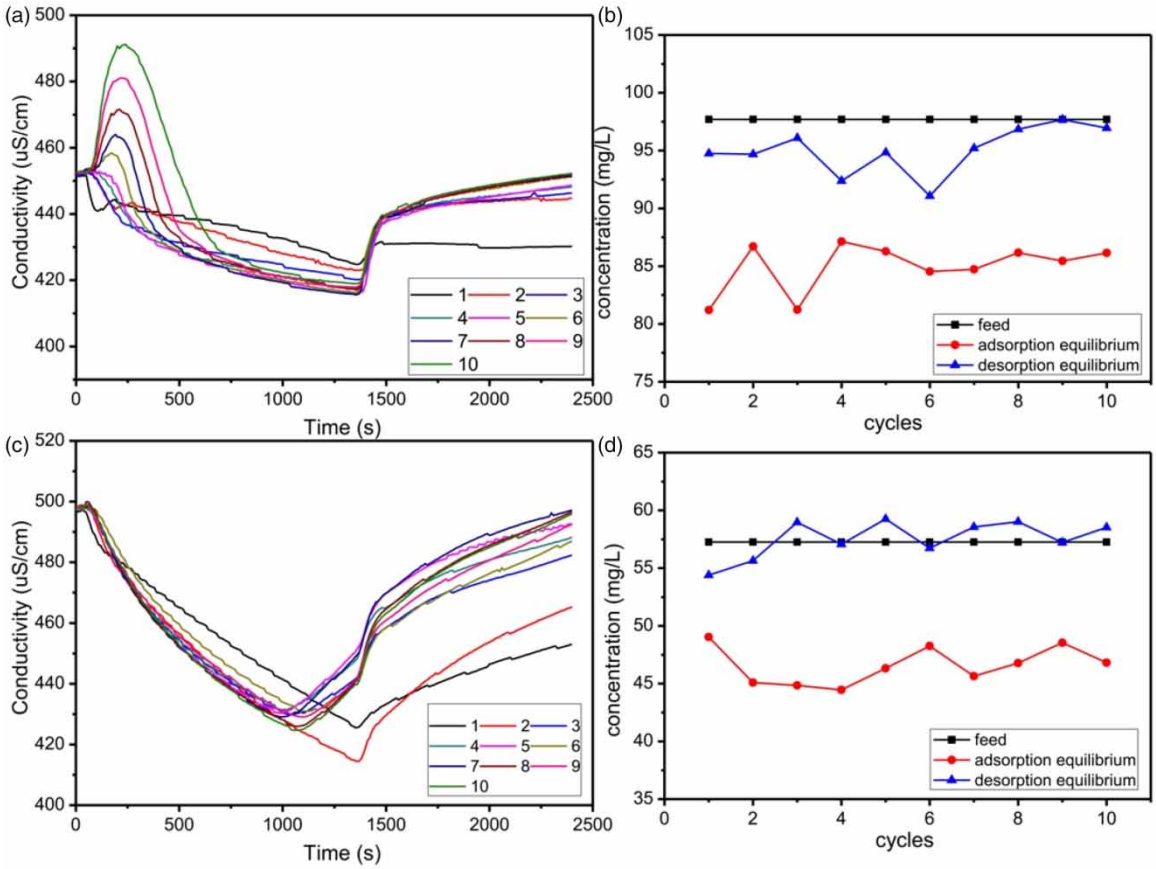

Figure 10 | The variation of conductivity and concentration in $CaCl_2$ (a) and (b) and $MgCl_2$ (c) and (d) solutions.

sensitive to the change of pH could form easily on electrodes, which would encourage Ca^{2+} to accumulate on electrodes leading to co-ion repulsion (Mossad & Zou 2013).

Variations of $MgCl_2$ concentration without organic substances are shown in Figure 11. Compared to S6, in S7 co-ion repulsion happened (Figure 11(a)). However, the co-ion repulsion was not obvious in SA solution (Figure 11(b)). These results suggest that in $MgCl_2$ solutions HA could make co-ion repulsion serious, which was similar to that in NaCl solutions. Salt adsorption efficiencies are shown in Figure 11(c), and it can be seen that Mg^{2+} adsorption in S6 was higher than that in S7. Different from Na^+, divalent ions Mg^{2+} would interact with HA through complex formation caused by acidic functional groups on HA,

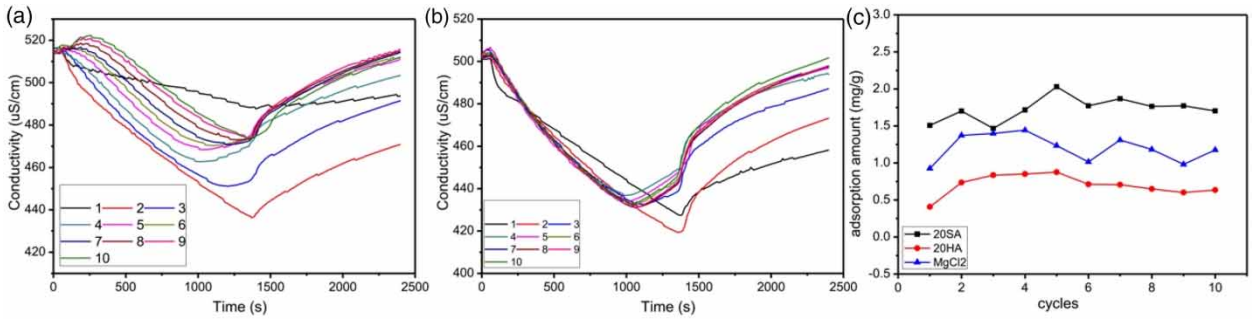

Figure 11 | The variation of conductivity and the adsorption amount of Mg^{2+} in different solutions: conductivity in (a) S7, (b) S8 and (c) adsorption amount.

which is called metal–humic complexes' effect (Alberts & Filip 1998). Mg^{2+} was able to form 'inner sphere' complexes. Owing to complexation, free magnesium ions available to be absorbed in water became less, leading to the decrease of adsorption amount (Topuz *et al.* 2012). In addition, from Figure 1, Mg^{2+} ions could neutralize the charge of HA molecules. The adsorbed molecules produced fewer charges. In the regeneration step, electrodes would adsorb fewer ions than in NaCl solution. Co-ion repulsion is also weakened. Some humic molecules will gather on electrodes. These macromolecules could lower the mobility of ions and block some pores on the electrodes. As a result, the salt adsorption amount in S7 is lower than that in S6. In pure solution, the Mg^{2+} adsorption amount was from 1.443 mg/g to 0.927 mg/g. In SA solution the adsorption amount was from 2.029 mg/g to 1.508 mg/g. It can be seen that in ten cycles, SA in water could help the adsorption of Mg^{2+}. Magnesium ions could interact with alginate resulting in ionic bridges (Topuz *et al.* 2012). Experimental results in this work showed that alginate absorbed by electrodes would bind magnesium ions and SA leading to increasing adsorption amount. In addition, SA is a kind of hydrophilic substance (Yan & Bai 2005). Mg-alginate gel attached on electrodes could decrease the hydrophobicity of electrodes to help salt removal (Fang *et al.* 2016).

In $CaCl_2$ solutions (Figure 12), adsorption in S9 was from 1.885 mg/g to 1.207 mg/g. In S10, the adsorption decreased to 1.010 mg/g to 0.483 mg/g. In S11, the adsorption amount was from 3.084 mg/g to 1.162 mg/g. Ca^{2+} and Mg^{2+} were similar ions, and both of them could complex with the negatively charged organic substances. But Ca^{2+} and alginate could interact with each other quickly (in a few minutes) and formed a stable gel with 'egg-box' structure (Lee & Mooney 2012). The bounds between calcium and alginate were firmer than those between magnesium and alginate (Topuz *et al.* 2012). The Ca-alginate could form a gel-like layer, which could not only lower the mobility of Ca^{2+} but also affect the structure of pores on electrodes. Thus, in the tenth cycle, the adsorption amount sharply decreased. ζ-potential of SA-Ca was lower than that of HA-Mg. Ca-SA gel could quickly accumulate on electrodes. Although SA could help the CDI adsorption amount, after long-time operation, gel would still accumulate on electrodes leading to fouling and reduce the adsorption amount.

CDI efficiency with organic fouling electrodes

From Figures 11 and 12, some organic substances in water might help increase the adsorption of divalent ions. To investigate the mechanism of the interaction between Mg^{2+} and Ca^{2+} and organic substances during the CDI process, the adsorption of Mg^{2+} and Ca^{2+} by the electrodes prefouled by organic substances is shown in Figure 13. In HA solutions and HA-fouled electrodes, the adsorption of Mg^{2+} is 1.036 mg/g–0.682 mg/g by 2 h HA-fouling electrodes and 0.437 mg/g–0.224 mg/g by 10 h-fouling electrodes. The adsorption amount of Ca^{2+} is nearly 0 mg/g. These results showed that HA adsorbed on electrodes only had an adverse influence on the adsorption amount of electrodes. When the fouling time increased the adsorption amount decreased. Apart from interaction and competition adsorption between ions and HA, HA would form a fouling layer on the electrodes. Adsorbed HA hindered transport of ions into pores of electrodes leading to the decrease of ions adsorption amount. It could be observed that the adsorption

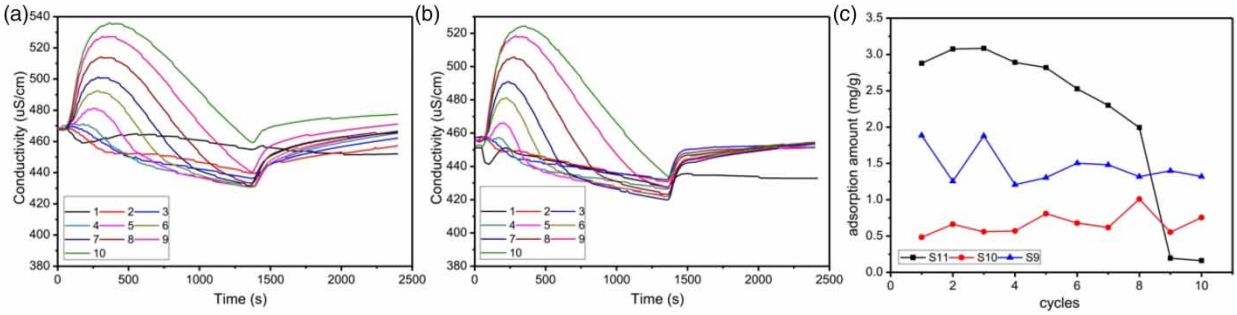

Figure 12 | The variation of conductivity and the adsorption amount of Ca^{2+} in different solutions: conductivity in (a) S10, (b) S11 and (c) adsorption amount.

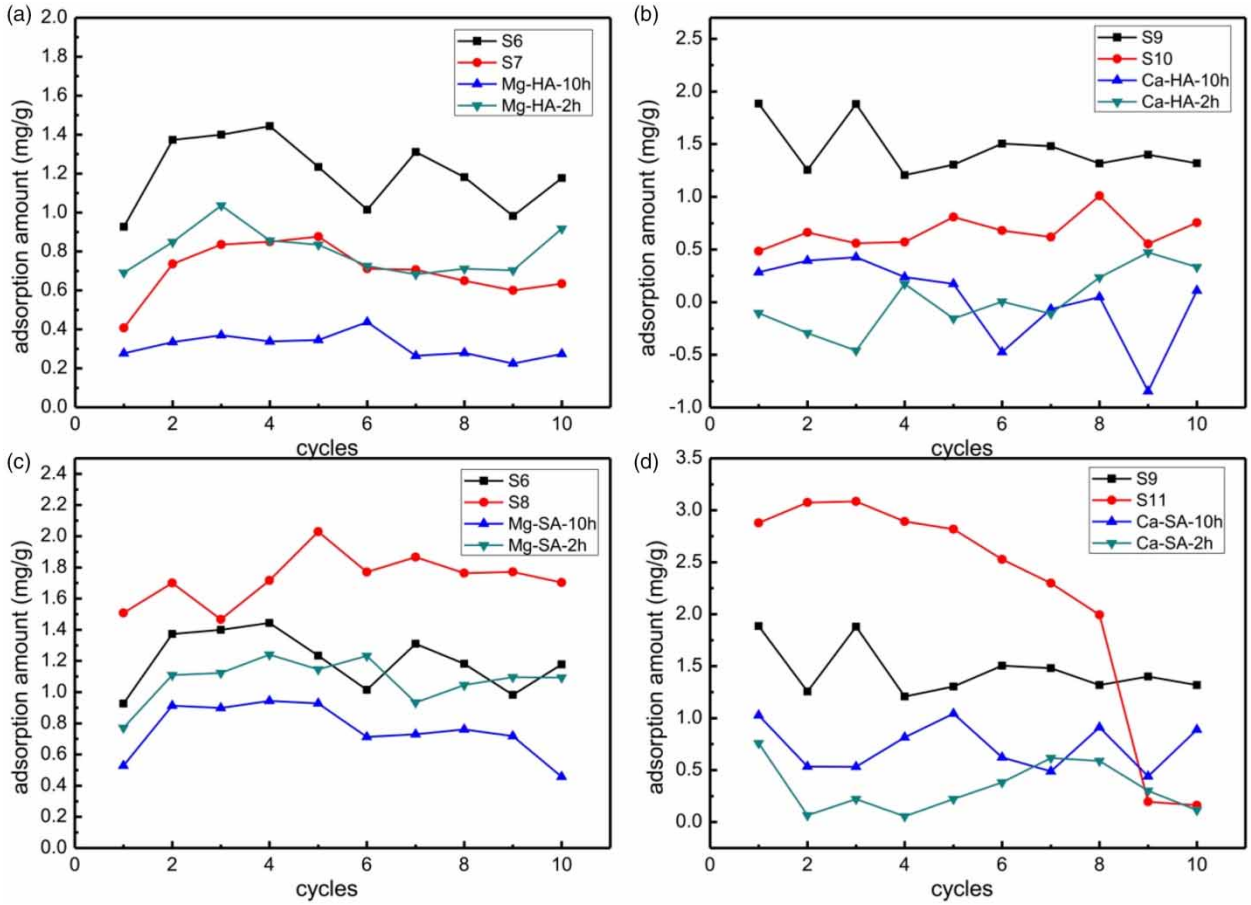

Figure 13 | Adsorption amount of Mg^{2+} and Ca^{2+} by organic fouling electrodes.

amount by 10 h-fouling electrodes is lower than that by 2 h-fouling electrodes.

In terms of SA fouling electrodes, the adsorption of Mg^{2+} was 1.241 mg/g–0.771 mg/g by 2 h-fouling electrodes, and 0.944 mg/g–0.457 mg/g by 10 h-fouling electrodes. The adsorption amount of Ca^{2+} was 0.759 mg/g–0.054 mg/g by 2 h-fouling electrodes and 1.044 mg/g–0.440 mg/g by 10 h-fouling electrodes. In $CaCl_2$ solution, 10 h-fouling electrodes adsorbed more Ca^{2+} ions than did 2 h-fouling electrodes. The increase of adsorption amount of ions was actually owing to SA on electrodes (Yoon *et al.* 2016). 10 h-fouling electrodes attracted more alginate. Bounds between calcium and alginate were more stable than between magnesium and alginate. These results proved that even alginate sodium could help increase adsorption by complexing divalent ions, the promotion depended on cations in water. If the interaction between the cations and organic substances was not strong enough to overcome the adverse impact of foulants on electrodes, efficiency of CDI would still decrease.

Electrochemical characteristics of electrodes

The CDI performance of the electrodes in different solutions was evaluated by cyclic voltammetry, as shown in Figure 14. Clearly, no evident oxidation/reduction peak could be seen in CV curves. This revealed that ions adsorption on electrodes was mainly caused by electrostatic interaction instead of Faradic reaction in solutions with organic substances. The specific capacitance could represent the double-layer capacitance of electrodes. According to previous reports, an ideal double-layer capacitor could exhibit a rectangular shape. The curves in Figure 14 were distorted. To exhibit a perfect CV curve, materials should have structure with abundant mesopores. Ions could enter into mesopores and form

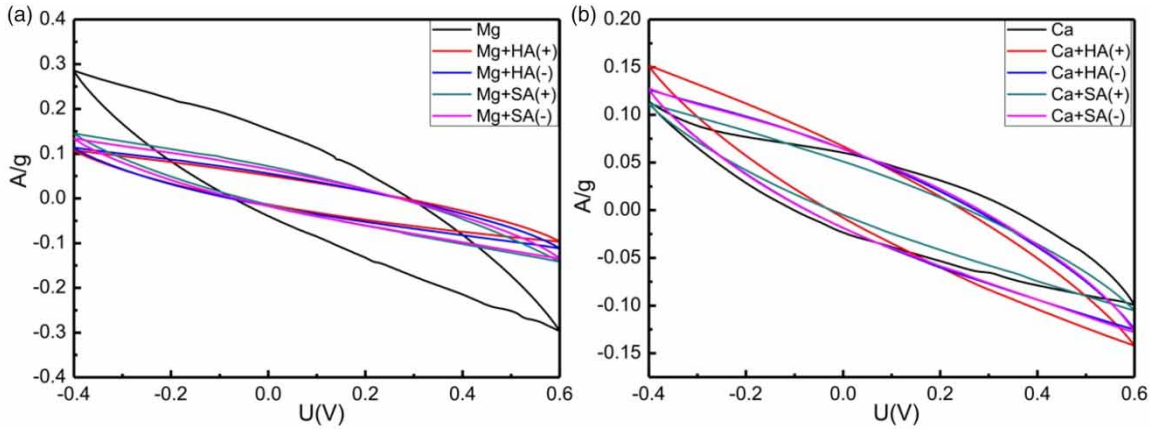

Figure 14 | CV curves of fresh and organic fouled electrodes in 5 mM $MgCl_2$ or $CaCl_2$ and 20 mg/L organic matter solutions. Positive and negative signs represent the polarities of electrodes fouled in solutions before electrochemical tests.

EDLs and EDLs would not overlap in mesopores (Hou & Huang 2013). Electrodes here belonged to microporous materials. Moreover, organic substances in water affected ion transport near the surface of electrodes. Symmetry in profiles meant that adsorption and desorption of salts were efficient without any chemical reactions.

The specific capacitance of those electrodes was calculated. In $MgCl_2$ solutions, electrodes had the specific capacitance of 1.39 F/g. In solutions with HA, the specific capacitance of positive and negative electrodes for both was 0.60 F/g. The positive and negative electrodes had the specific electrodes of 0.47 F/g and 0.52 F/g with SA, respectively. In $CaCl_2$ solutions, the specific capacitance of clean electrodes was 0.59 F/g. Positive and negative electrodes in HA solution had the capacitance of 0.54 F/g and 0.58 F/g, respectively. In SA solutions, the capacitance of positive and negative electrodes was 0.4 F/g and 0.59 F/g. The specific capacitance of fouled electrodes is lower than clean ones. The reduction of specific capacitance was due to a decreased amount of micropores and mesopores of electrodes. It proved that both SA and HA affected the formation of EDLs. They decreased the pores on electrodes and hindered the ion transport.

Effect of organic fouling on energy consumption

Energy consumption efficiency in $CaCl_2$ and $MgCl_2$ is shown in Figure 15. It can be seen that due to an increase of adsorption amount, energy consumption in SA was lower than that in pure and HA solution. In SA solution, the adsorption amount increased because of the complexation between alginate and divalent ions. However, complexation led to the formation of alginate gel; in particular, Ca-alginate gel was very stable. After ten cycles of the CDI process, the gel accumulated on electrodes. Then, some Ca-alginate complexes could accumulate on electrodes hindering ions entering the pores of activated carbon and increasing the resistance of electrodes. This interaction made energy consumption efficiency rise sharply at the tenth cycle.

In view of the energy consumption analysis, it is necessary to take action to remove organic substances. Analysis of influent water must be carried out to figure out the kind of organic substances and ions.

CONCLUSION

In this study, we systematically investigated the role of organic substances on CDI fouling by varying the ion compositions of the feed solution. The adsorption efficiency and energy consumption were studied in diverse feed solutions. We obtained the following conclusions:

(1) During CDI operation, in NaCl solutions, both SA and HA could influence deionization. With the concentration of organics increasing, the adsorption amount of ions decreased. Organic substances were adsorbed on electrodes and hardly desorbed. There existed adsorption competition between organics and ions.

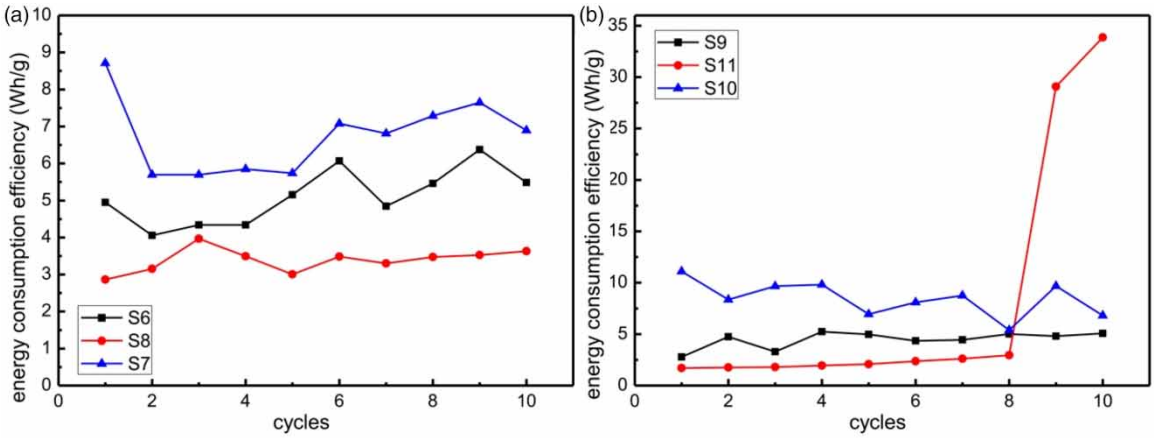

Figure 15 | Energy consumption efficiency in $CaCl_2$ and $MgCl_2$ solutions.

(2) In addition, adsorbed organic molecules caused serious co-ion repulsion during the CDI process, decreasing the efficiency of the adsorption amount and energy consumption.
(3) In $MgCl_2$ and $CaCl_2$ solutions, the adsorption amount was also affected by organic substances. Adsorption of Ca^{2+} and Mg^{2+} with the absence of organic matter was at a stable stage.
(4) In SA fouling, the adsorption amount was increased because of the complexation between SA and divalent ions. Alginate and Ca^{2+} and Mg^{2+} can interact and formed Ca-alginate and Mg-alginate gel. Alginate acted as binding bridges connecting electrodes and ions. However, after long-time operation, complexation gel would accumulate on electrodes, reducing the efficiency of the CDI device.

ACKNOWLEDGEMENTS

This work was supported by the National Natural Science Foundation of China (No. 51908181&No.51678187), the Natural Science Foundation of Hebei Province (No. E2019202011 and No. E2019202012), and the Natural Foundation of Tianjin (No. 19JCJQJC63000).

DATA AVAILABILITY STATEMENT

All relevant data are included in the paper or its Supplementary Information.

REFERENCES

Alberts, J. J. & Filip, Z. 1998 Metal binding in estuarine humic and fulvic acids: FTIR analysis of humic acid-metal complexes. *Environmental Technology* **19**, 923–931.

Alfredy, T., Jande, Y. A. C. & Pogrebnaya, T. 2019 Removal of lead ions from water by capacitive deionization electrode materials derived from chicken feathers. *Journal of Water Reuse and Desalination* **9**, 282–291.

Chen, L., Wang, C., Liu, S., Hu, Q., Zhu, L. & Cao, C. 2018 Investigation of the long-term desalination performance of membrane capacitive deionization at the presence of organic foulants. *Chemosphere* **193**, 989–997.

Choi, S., Chang, B., Kang, J. H., Diallo, M. S. & Choi, J. W. 2017 Energy-efficient hybrid FCDI-NF desalination process with tunable salt rejection and high water recovery. *Journal of Membrane Science* **541**, 580–586.

Dykstra, J. E., Zhao, R., Biesheuvel, P. M. & van der Wal, A. 2016 Resistance identification and rational process design in capacitive deionization. *Water Research* **88**, 358–370.

Fang, C., Liu, P., Chung, L., Shao, H., Ho, C., Chen, R., Fan, H., Liang, T., Chang, M. & Horng, R. 2016 A flexible and hydrophobic polyurethane elastomer used as binder for the activated carbon electrode in capacitive deionization. *Desalination* **399**, 34–39.

Hou, C. & Huang, C. 2013 A comparative study of electrosorption selectivity of ions by activated carbon electrodes in capacitive deionization. *Desalination* **314**, 124–129.

Lee, K. Y. & Mooney, D. J. 2012 Alginate: properties and biomedical applications. *Progress in Polymer Science* **37**, 106–126.

Li, F., Yuasa, A., Ebie, K., Azuma, Y., Hagishita, T. & Matsui, Y. 2002 Factors affecting the adsorption capacity of dissolved organic matter onto activated carbon: modified isotherm analysis. *Water Research* **36**, 4592–4604.

Liu, X., Whitacre, J. F. & Mauter, M. S. 2018 Mechanisms of humic acid fouling on capacitive and insertion electrodes for

electrochemical desalination. *Environmental Science and Technology* **52**, 12633–12641.

Lu, D., Cai, W. & Wang, Y. 2017 Optimization of the voltage window for long-term capacitive deionization stability. *Desalination* **424**, 53–61.

Mossad, M. & Zou, L. 2013 Study of fouling and scaling in capacitive deionisation by using dissolved organic and inorganic salts. *Journal of Hazardous Materials* **244–245**, 387–393.

Shapira, B., Avraham, E. & Aurbach, D. 2016 Side reactions in capacitive deionization (CDI) processes: the role of oxygen reduction. *Electrochimica Acta* **220**, 285–295.

Tang, W., Zeng, G., Gong, J., Liang, J., Xu, P., Zhang, C. & Huang, B. 2014 Impact of humic/fulvic acid on the removal of heavy metals from aqueous solutions using nanomaterials: a review. *Science of the Total Environment* **468–469**, 1014–1027.

Topuz, F., Henke, A., Richtering, W. & Groll, J. 2012 Magnesium ions and alginate do form hydrogels: a rheological study. *Soft Matter* **8**, 4877.

Tsai, Y. & Doong, R. 2015 Activation of hierarchically ordered mesoporous carbons for enhanced capacitive deionization application. *Synthetic Metals* **205**, 48–57.

Wang, G., Pan, C., Wang, L., Dong, Q., Yu, C., Zhao, Z. & Qiu, J. 2012 Activated carbon nanofiber webs made by electrospinning for capacitive deionization. *Electrochimica Acta* **69**, 65–70.

Xie, J., Liu, X., Shen, M., Nie, S., Zhang, H., Li, C., Gong, D. & Xie, M. 2013 Purification, physicochemical characterisation and anticancer activity of a polysaccharide from Cyclocarya paliurus leaves. *Food Chemistry* **136**, 1453–1460.

Xu, H., de Koning, J. & Geng, Y. 2019 Reliability and efficiency of an advanced tertiary treatment process for wastewater reclamation. *Journal of Water Reuse and Desalination* **9**, 385–395.

Yan, W. L. & Bai, R. 2005 Adsorption of lead and humic acid on chitosan hydrogel beads. *Water Research* **39**, 688–698.

Yang, K. & Xing, B. 2009 Adsorption of fulvic acid by carbon nanotubes from water. *Environmental Pollution* **157**, 1095–1100.

Yang, S., Hu, J., Chen, C., Shao, D. & Wang, X. 2011 Mutual effects of Pb(II) and humic acid adsorption on multiwalled carbon nanotubes/polyacrylamide composites from aqueous solutions. *Environmental Science and Technology* **45**, 3621–3627.

Yoon, H., Lee, J., Kim, S., Kang, J., Kim, S., Kim, C. & Yoon, J. 2016 Capacitive deionization with Ca-alginate coated-carbon electrode for hardness control. *Desalination* **392**, 46–53.

Zhu, Z., Peng, D. & Wang, H. 2019 Seawater desalination in China: an overview. *Journal of Water Reuse and Desalination* **9**, 115–132.

First received 31 October 2020; accepted in revised form 31 December 2020. Available online 4 February 2021